AD-A174 397 AN ANALYTICAL MODEL OF AN IMPULSIVE THRUSTER(U) ARMY 1/1
ARMAMENT RESEARCH AND DEVELOPMENT CENTER DOVER NJ
ARMAMENT ENGINEERING DIRECTORATE E M FRIEDMAN ET AL
UNCLASSIFIED NOV 86 ARAED-TR-86034 F/G 19/1 NL

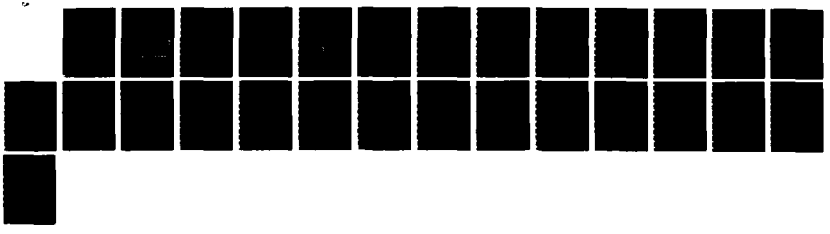

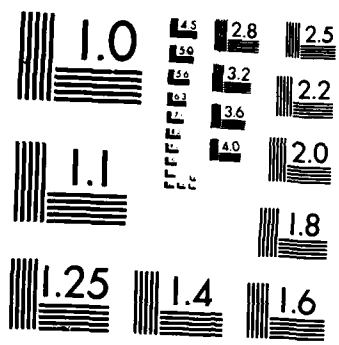

(12)

AD-A174 397

AD

AD-E401 601

TECHNICAL REPORT ARAED-TR-86034

AN ANALYTICAL MODEL OF AN IMPULSIVE THRUSTER

EUGENE M. FRIEDMAN
MICHAEL J. AMORUSO
ROMEL CAMPBELL

NOVEMBER 1986

US ARMY ARMAMENT MUNITIONS & CHEMICAL COMMAND
ARMAMENT RDE CENTER

U. S. ARMY ARMAMENT RESEARCH, DEVELOPMENT AND ENGINEERING CENTER
ARMAMENT ENGINEERING DIRECTORATE
DOVER, NEW JERSEY

The views, opinions, and/or findings contained in this report are those of the author(s) and should not be construed as an official Department of the Army position, policy, or decision, unless so designated by other documentation.

Destroy this report when no longer needed by any method that will prevent disclosure of contents or reconstruction of the document. Do not return to the originator.

UNCLASSIFIED

SECURITY CLASSIFICATION OF THIS PAGE (When Data Entered)

REPORT DOCUMENTATION PAGE		READ INSTRUCTIONS BEFORE COMPLETING FORM
1. REPORT NUMBER Technical Report ARAED-TR-86034	2. GOVT ACCESSION NO.	3. RECIPIENT'S CATALOG NUMBER
4. TITLE (and Subtitle) AN ANALYTICAL MODEL OF AN IMPULSIVE THRUSTER		5. TYPE OF REPORT & PERIOD COVERED Final 6. PERFORMING ORG. REPORT NUMBER
7. AUTHOR(s) Eugene M. Friedman Michael J. Amoruso Romel Campbell		8. CONTRACT OR GRANT NUMBER(s)
9. PERFORMING ORGANIZATION NAME AND ADDRESS ARDEC, AED Armaments Technology Div (SMCAR-AET-A) Dover, NJ 07801		10. PROGRAM ELEMENT, PROJECT, TASK AREA & WORK UNIT NUMBERS
11. CONTROLLING OFFICE NAME AND ADDRESS ARDEC, IMD STINFO Div (SMCAR-MSI) Dover, NJ 07801		12. REPORT DATE November 1986 13. NUMBER OF PAGES 27
14. MONITORING AGENCY NAME & ADDRESS(if different from Controlling Office)		15. SECURITY CLASS. (of this report) Unclassified 15a. DECLASSIFICATION/DOWNGRADING SCHEDULE

16. DISTRIBUTION STATEMENT (of this Report)

Approved for public release; distribution unlimited.

17. DISTRIBUTION STATEMENT (of the abstract entered in Block 20, if different from Report)

18. SUPPLEMENTARY NOTES

19. KEY WORDS (Continue on reverse side if necessary and identify by block number)

Flight simulation
Analytical simulation
Impulsive thruster

20. ABSTRACT (Continue on reverse side if necessary and identify by block number)

The use of impulsive or nearly impulsive thrusters for the maneuvering force on artillery projectiles has recently been of great interest. The computational cost of numerically integrating the force and torque of distributed thrusters has been high. A method is developed for the one-step application of an exact solution of the flight mechanics for a helical thruster distribution on an axisymmetric body.

DD FORM 1 JAN 73 1473 EDITION OF 1 NOV 65 IS OBSOLETE

UNCLASSIFIED

SECURITY CLASSIFICATION OF THIS PAGE (When Data Entered)

ACKNOWLEDGMENT

The authors wish to express their appreciation to Walter Koenig whose efforts contributed immeasurably to the success of this method.

CONTENTS

	Page
Introduction	1
Analysis	1
Numerical Example	10
Conclusions	10
Symbols	15
Appendix - Program CGSP	17
Distribution List	23

INTRODUCTION

A great deal of interest has been shown within the Army in recent years in gun fired projectiles which correct their flight paths by impulsive means. One of the more interesting concepts for large caliber projectiles has been an arrangement of propellant-filled helical grooves on the cylindrical portion of the projectile which burn in a progressive manner (from one end to the other). This arrangement has the virtue of controlling the introduction of nutation and precession motion to the flight.

In the flight simulation of such projectiles, the burning of the propellant has historically been modeled as the application of a radial force to the projectile which moves from one end of the groove to the other as the point of burning of the propellant moves. Since the typical speed of burning might be 20,000 feet per second, the integration step size (in time) required to adequately model the shape of the helical groove in space will be quite short compared to the typical rigid body aerodynamic response times of the projectile, causing very large costs in computer time in the flight simulation of the projectile. Therefore, an impulsive analytical model of such a burning process was developed which exactly models the dynamic response of a rigid axisymmetric body to which is applied a radial thrust, moving from one end to the other with a finite burn time. This process is applied as a single step change in the spin components in body fixed coordinates, resulting in large savings in computer time compared to the numerical integration of the rigid body response. This is not an approximation to the rigid body motion under this force alone, but an exact solution; the numerical solution is an approximation to the geometry of the helix. If there is an approximation, it is in the neglect of the aerodynamic forces during the burn time. Aerodynamic forces typically provide approximately two g's of acceleration which is almost entirely axial, while the impulsive thruster typically provides three thousand radial g's during the short duration of the burn. This would appear to amply justify neglect of the lateral aerodynamics during the short application time of the impulse.

ANALYSIS

The Euler equations of rotational motion of a rigid body can be written as

$$I_x \dot{w}_x - w_y w_z (I_y - I_z) = N_x = 0 \tag{1}$$

$$I_y \dot{w}_y - w_z w_x (I_z - I_x) = N_y = (\bar{x} + \Delta x)\ F \cos(\theta) \tag{2}$$

$$I_z \dot{w}_z - w_x w_y (I_x - I_y) = N_z = (\bar{x} + \Delta x)\ F \sin(\theta) \tag{3}$$

where $N_x = 0$, since the applied force is radial and exerts no torque about the x-axis, and $I_y - I_z = 0$ since the body is assumed axially symmetric (fig. 1). The

moment arm due to the instantaneous application of the force of the burning propellant is at $\bar{x} + \Delta x$, where Δx is the displacement between the initiation point of ignition and the center of mass of projectile, and $\bar{x} = 0$ at the point of initiation of the burning of the propellant.

Several auxiliary relationships are required for this development (fig. 2). Inspection of this figure reveals that

$$\bar{t} = t - t_o \tag{4}$$

$$\bar{x} = x - x_M + \Delta x = x - x_o \tag{5}$$

$$\bar{\theta} = (\theta - \theta_0) = 2 \pi \bar{T}\bar{x}/D \tag{6}$$

$$\bar{l}^2 = \{ \bar{x}^2 + (r\bar{\theta})^2 \}^{1/2} \tag{7}$$

$$\bar{l} = -\bar{x} [1 + (\pi T)^2]^{1/2} \tag{8}$$

where $\bar{l}$ is the distance down the groove, x_o is the value of x at the start of the burn, and $\bar{x}$ is zero at the start of the burn. Similarly, $\bar{t}$ and $\bar{\theta}$ are both zero at the start of burn. The quantity x_M is the value for x at the center of mass and Δx is the displacement in x between the center of mass and the start of thruster burn. Note from equation 5 that $\bar{x} + \Delta x = x - x_M$.

If the linear burning rate of the propellant is R feet per second, and it yields I pound-seconds of thrust per foot of thruster, then

$$F = RI \tag{9}$$

is the force of thrust being applied to the groove at the point of burning at any time during the burning process.

From equation 6

$$d\bar{x}/dt = -[D/(2\pi T)]\, d\bar{\vartheta}/dt \tag{10}$$

From equation 8

$$d\bar{l}/dt = -d\bar{x}/dt \sqrt{(1 + (\pi T)^2)} \tag{11}$$

but

$$d\bar{l}/dt = R \tag{12}$$

where R is the linear burning rate.

From equation 1

$$dw_x = 0 \tag{13}$$

for an axially symmetric projectile.

From equation 8

$$\bar{x} = -\bar{l}/\sqrt{[1 + (\pi T)^2]} = -R\bar{t}/\sqrt{[1 + (\pi T)^2]} \tag{14}$$

From equations 6 and 14

$$\bar{\theta} = \theta - \theta_0 = +2\pi T\bar{x}/D = -2\pi RT\bar{t}/\{D\sqrt{[1 + (\pi T)^2]}\} \tag{15}$$

Thus, when equations 9, 14, and 15 are applied, equations 2 and 3 become

$$I_y\dot{w}_y - w_z w_x(I_z - I_x) = \{-R\bar{t}/\sqrt{[1 + (\pi T)^2]} + \Delta x\}*RI* \cos\{-2\pi TR\bar{t}/[D*\sqrt{(1 + (\pi T)^2)}] + \theta_0\} \tag{16}$$

$$I_z\dot{w}_z - w_x w_y(I_x - I_y) = \{-R\bar{t}/\sqrt{[1 + (\pi T)^2]} + \Delta x\}*RI* \sin\{-2\pi TR\bar{t}/[D*\sqrt{(1 + (\pi T)^2)}] + \theta_0\} \tag{17}$$

Define

$$A = -R^2 I/\sqrt{(1 + (\pi T)^2]} \tag{18}$$

$$B = R\ I\Delta\ x \tag{19}$$

and

$$K = -2\pi TR/\{D*\sqrt{(1 + (\pi T)^2)}] \tag{20}$$

then equations 16 and 17 become

$$I_y\dot{w}_y - w_z w_x(I_z - I_x) = [A\bar{t} + B]\cos(K\bar{t} + \theta_0) \tag{21}$$

$$I_z\dot{w}_z - w_y w_x(I_x - I_y) = [A\bar{t} + B]\sin(K\bar{t} + \theta_0) \tag{22}$$

Equations 21 and 22 can be decoupled by differentiating each and substituting the solution for $\dot{w}_z$ from 22 into the derivative of 21 and the solution for $\dot{w}_y$ from 21 into the derivative of 22. Keeping in mind that $\dot{w}_x = 0$, the differentiation results in

$$I_y\ddot{w}_y - \dot{w}_z w_x(I_z - I_x) = A\cos(K\bar{t} + \theta_0) - AK\bar{t}\sin(K\bar{t} + \theta_0)$$
$$- BK\sin(K\bar{t} + \theta_0) \tag{23}$$

$$I_z\ddot{w}_z - \dot{w}_y w_x(I_x - I_y) = A\sin(K\bar{t} + \theta_0) + AK\bar{t}\cos(K\bar{t} + \theta_0)$$
$$+ BK\cos(K\bar{t} + \theta_0) \tag{24}$$

The substitution of the solution of 22 into 23 eliminates $\dot{w}_z$

$$I_y\ddot{w}_y + w_x^2 w_y(I_x - I_z)(I_x - I_y)/(I_z) =$$
$$\{A\bar{t}[w_x(I_z - I_x)/(I_z) - K] + B[w_x(I_z - I_x)/(I_z) - K]\}$$
$$\sin(K\bar{t} + \theta_0) + A\cos(K\bar{t} + \theta_0) \tag{25}$$

while the substitution of the solution of 21 into 24 eliminates $\dot{w}_y$

$$I_z\ddot{w}_z + w_x^2 w_z(I_x - I_z)(I_x - I_y)/(I_y) =$$
$$\{A\bar{t}[w_x(I_x - I_y)/(I_y) + K] + B[w_x(I_x - I_y)/(I_y) + K]\}$$
$$\cos(K\bar{t} + \theta_0) + A\sin(K\bar{t} + \theta_0) \tag{26}$$

For convenience, rewrite 25 as

$$J\ddot{w}_y + Mw_y = (E\bar{t} + F)\sin(K\bar{t} + \theta_0) + A\cos(K\bar{t} + \theta_0) \tag{27}$$

where

$$J = I_y \tag{28}$$

$$M = w_x^2(I_x - I_z)\,(I_x - I_y) / (I_z) \tag{29}$$

$$E = -A[K + w_x(I_x - I_z) / (I_z)] \tag{30}$$

and

$$F = -B[K + w_x(I_x - I_z) / (I_z)] \tag{31}$$

The complete solution to 27 is the sum of the general solution of the equation with the driving terms set to zero and a particular solution of the inhomogeneous equation. The general solution of the homogeneous equation

$$J\ddot{w}_y + Mw_y = 0$$

$$w_y = c_h \cos(\lambda\bar{t} + \phi) \tag{32}$$

which, if substituted back into the homogeneous equation, yields the secular equation

$$-\lambda^2 J + M = 0 \tag{33}$$

or

$$\lambda = \sqrt{(M/J)} \tag{34}$$

A particular solution of the inhomegeneous equation is needed. Try an expression of the form

$$w_y = c_1 \sin(K\bar{t} + \theta_0) + c_2\cos(K\bar{t} + \theta_0) + c_3\bar{t} \sin(K\bar{t} + \theta_0)$$
$$+ c_4\bar{t} \cos(K\bar{t} + \theta_0) \tag{35}$$

Differentiate 35 twice to obtain $\ddot{w}_y$, then substitute it and 35 into 27 to evaluate c_1, c_2, c_3, and c_4. We get

$$-c_1K^2J - 2c_4KJ + Mc_1 = F \tag{36}$$

$$-c_3K^2J + Mc_3 = E \tag{37}$$

$$-c_2K^2J + 2c_3KJ + c_2M = A \tag{38}$$

$$-c_4K^2J + Mc_4 = 0 \tag{39}$$

From 39, if $J K^2 - M \neq 0$, (i.e., $K \neq \lambda$, cf. equation 33)

$$c_4 - 0 \tag{40}$$

From 40 and 36,

$$Mc_1 - JK^2 c_1 = F$$

or using 34 to eliminate M

$$c_1 = F / (M - JK^2) = F / [J(\lambda^2 - K^2)] \tag{41}$$

From 37

$$c_3 = E / (M - K^2J) = E / [J (\lambda^2 - K^2)] \tag{42}$$

From 38 and 42

$$c_2 = [A (\lambda^2 - K^2) - 2KE] / [J (\lambda^2 - K^2)^2] \tag{43}$$

Therefore 35 simplifies to

$$w_y = c_1 \sin(K\bar{t} + \vartheta_0) + c_2 \cos(K\bar{t} + \vartheta_0) + c_3 \bar{t} \sin(K\bar{t} + \vartheta_0) \tag{44}$$

and the complete solution is the sum of 44 and 32

$$w_y = c_h \cos(\lambda\bar{t} + \phi) + c_1 \sin(K\bar{t} + \vartheta_0) + c_2 \cos(K\bar{t} + \vartheta_0)$$

$$+ c_3 \bar{t} \sin(K\bar{t} + \vartheta_0)$$

which can be rewritten as

$$w_y = c_5\cos(\lambda\bar{t}) + c_6\sin(\lambda\bar{t}) + c_1\sin(K\bar{t} + \theta_0) + c_2\cos(K\bar{t} + \theta_0)$$
$$+ c_3\bar{t}\,\sin(K\bar{t} + \theta_0) \tag{45}$$

The constants of integration c_5 and c_6 can be evaluated in terms of the initial conditions w_{y_0} and $\dot{w}_{y0}$. Recall that c_1, c_2, and c_3 are already determined; see 41, 42, and 43.

$$w_{y0} = w_{y0}[t = t_c - L/(2R)] = w_{y0}[\bar{t} = 0] \tag{46}$$

$$\dot{w}_{y0} = \dot{w}_{y0}[t = t_c - L/(2R)] = \dot{w}_{y0}(\bar{t} = 0] \tag{47}$$

where t_c is the center time, the time of the middle of the burn. For convenience, make the definition

$$\tau = L/R \tag{48}$$

which is the burn time of a thruster. Thus the initial conditions become

$$w_{y0} = w_{y0}(t = t_c - \tau/2) = w_{y0}(\bar{t} = 0) \tag{49}$$

$$\dot{w}_{y0} = \dot{w}_{y0}(t = t_c - \tau/2) = \dot{w}_{y0}(\bar{t} = 0) \tag{50}$$

The derivative of 45 is

$$\dot{w}_y(\bar{t}) = -\lambda c_5\sin(\lambda\bar{t}) + \lambda c_6\cos(\lambda\bar{t}) + Kc_1\cos(K\bar{t} + \theta_0)$$
$$- Kc_2\sin(K\bar{t} + \theta_0) + c_3\sin(K\bar{t} + 0_0) + c_3K\bar{t}\,\cos(K\bar{t} + \theta_0) \tag{51}$$

Thus, at $t = t_c - \tau/2$, or $\bar{t} = 0$

$$w_{y0} = c_5 + c_1\sin[\theta_0] + c_2\cos[\theta_0] \tag{52}$$

and

$$\dot{w}_{yo} = \lambda c_6 + Kc_1\cos[\theta_0] - Kc_2\sin[\sin\theta_0] + c_3\sin[\theta_0] \tag{53}$$

Solving for c_6 from 53

$$c_6 = [1/\lambda] \{\dot{w}_{yo} - Kc_1\cos[\theta_o] + Kc_2\sin[\theta_o] - c_3\sin[\theta_o] \} \quad (54)$$

Solving 52 for c_5

$$c_5 = \{w_{y0} - c_1\sin[\theta_0] - c_2\cos(\theta_0) \} \quad (55)$$

Similarly, the solution to 26 is required

$$\bar{J}\ddot{w}_z + \bar{M} w_z = (\bar{E}t + \bar{F}) \cos(K\bar{t} + \theta_0) + A \sin(K\bar{t} + \theta_0) \quad (56)$$

where

$$\bar{J} = I_z = J (I_z/I_y) \quad (57)$$

$$\bar{M} = w_x^2 (I_x - I_z) (I_x - I_y) / I_y = M (I_z/I_y) \quad (58)$$

$$\bar{E} = A [K + w_x(I_x - I_y) / I_y] \quad (59)$$

$$\bar{F} = B [K + w_x(I_x - I_y) /I_y] \quad (60)$$

The homogeneous part of 56 is formally identical to the homogeneous part of 27; therefore the homogeneous solution of 56 is formally the same as the homogeneous solution of 27 which is expressed by 32 and 34. For the inhomogeneous solution, again try the form of 35

$$w_z = \bar{c}_1\sin(K\bar{t} + \theta_0) + \bar{c}_2\cos(K\bar{t} + \theta_0) + \bar{c}_3\bar{t} \sin(K\bar{t} + \theta_0) + \bar{c}_4\bar{t} \cos(K\bar{t} + \theta_0) \quad (61)$$

Similarly, differentiate twice and substitute into the differential equation, in this case 56, yielding

$$\bar{c}_1 = [A(\bar{M} - K \bar{J}) + 2\bar{J}K\bar{E}] / [\bar{M} - K^2\bar{J}]^2$$

or since $M/J = \bar{M}/\bar{J} = \lambda^2$, then

$$\bar{c}_1 = [A(\lambda^2 - K^2) + 2K\bar{E}] \; / \; [\bar{J}(\lambda^2 - K^2)^2] \tag{62}$$

$$\bar{c}_2 = \bar{F}/[\bar{M} - K^2\bar{J}] = \bar{F}/[\bar{J}(\lambda^2 - K^2)] \tag{63}$$

$$\bar{c}_3 = 0 \tag{64}$$

and

$$\bar{c}_4 = E/\ (M - K^2J) = \bar{E}/\ [\bar{J}(\lambda^2 - K^2)\ ] \tag{65}$$

which should be compared to 40 through 43. Following the pattern used to evaluate the constants of integration in equation 45, first write the recase complete solution of 56, which is analogous to 45, as

$$w_z = \bar{c}_5\cos(\lambda\bar{t}) + \bar{c}_6\sin(\lambda\bar{t}) + \bar{c}_1\sin(K\bar{t} + \theta_0) + \bar{c}_2\cos(K\bar{t} + \theta_0)$$
$$+ \bar{c}_4\bar{t}\cos\ (K\bar{t} + \theta_0) \tag{66}$$

where

$$\bar{c}_5 = \{w_{z0} - \bar{c}_1\sin[\theta_0] - \bar{c}_2\cos[\theta_0]\ \ \} \tag{67}$$

and

$$\bar{c}_6 = [1/\lambda]\ \{\dot{w}_{z\theta} - K\bar{c}_1\cos[\theta_0] + K\bar{c}_2\sin[\theta_0] - \bar{c}_4\cos[\theta_0]\ \} \tag{68}$$

To obtain the final result, evaluate 45 and 66 at $t = t_c - \tau/2$ or, equivalently, at $\bar{t} = \tau = L/R$.

$$w_y = c_5\cos[\lambda L/R] + c_6\sin(\lambda L/R] + c_1\sin[KL/R + \theta_0]$$
$$+ c_2\cos[KL/R + \theta_0] + c_3[L/R]\ \sin[KL/R + \theta_0] \tag{69}$$

$$w_z = \bar{c}_5\cos[\lambda L/R] + \bar{c}_6\sin[\lambda L/R] + \bar{c}_1\sin[KL/R + \theta_0]$$
$$+ \bar{c}_2\cos[KL/R + \theta_0] + \bar{c}_4[L/R]\ \cos[KL/R + \theta_0] \tag{70}$$

Care must be taken in specifying initial conditions. The original equations to be solved were the coupled first order equations 2 and 3. For these equations, only w_{yo} and w_{zo} need to be specified. However, when the equations are decoupled, the order is increased and the initial conditions, $\dot{w}_{yo}$ and $\dot{w}_{zo}$, are also required. These cannot be specified arbitrarily. Instead, to avoid spurious solutions and to assure consistency with the original coupled first order equations 2 and 3, $\dot{w}_{yo}$ and $\dot{w}_{zo}$ in principle must be calculated from w_{yo} and w_{zo} using equations 2 and 3. Equivalently, equations 21 and 22 can be solved for $\dot{w}_y$ and $\dot{w}_z$ with t set to zero to yield the required initial conditions, viz.

$$\dot{w}_{yo} = \{w_{zo} w_x [I_z - I_x] + B \cos \theta_o\} / I_y \tag{71}$$

$$\dot{w}_{zo} = \{w_{yo} w_x [I_x - I_y] + B \sin \theta_o\} / I_z \tag{72}$$

where B could be replaced by R $I\Delta x$. (See equation 19.) A program implementing this approach is in the appendix.

NUMERICAL EXAMPLE

The analytical approach described above was tested by comparison to numerical integration of equations 2 and 3 using a fourth order Runge-Kutta integration technique. These results are reported in table 1. The first entry is the exact result obtained by the analytical technique. The second entry represents numerical integration using an integration time step of 0.00000001 second. Results are interpolated to yield a value at the exact time of the end of burn. (If the simulations are adjusted to make them stop at the same time, the numerical and analytical results for w_y and w_z agree to at least eight significant figures.) The third and fourth table entries use integration time steps of 0.0000001 second and 0.000001 second, respectively. Note that the results obtained numerically required from 23 to 2085 times the computer CPU time as the new analytical approach to obtain 3 to 6 significant figure accuracy, respectively.

CONCLUSIONS

The closed form, analytical solution has been accurate and highly efficient for the simulation of the flight of projectiles with maneuvers implemented by helical, quasi-impulsive thrusters. The technique will be implemented in the further development of such projectiles at ARDEC.

Table 1. Comparison of results

Model type	Time step (sec)	CPU time (sec)	w_y (rad)	w_z (rad)
Analytical	N/A	0.0106	0.53275603	-0.41630908
Numerical	10^{-8}	22.096	0.53275601	-0.41630910
Numerical	10^{-7}	2.278	0.53275061	-0.41631581
Numerical	10^{-6}	0.246	0.53234719	-0.41681537

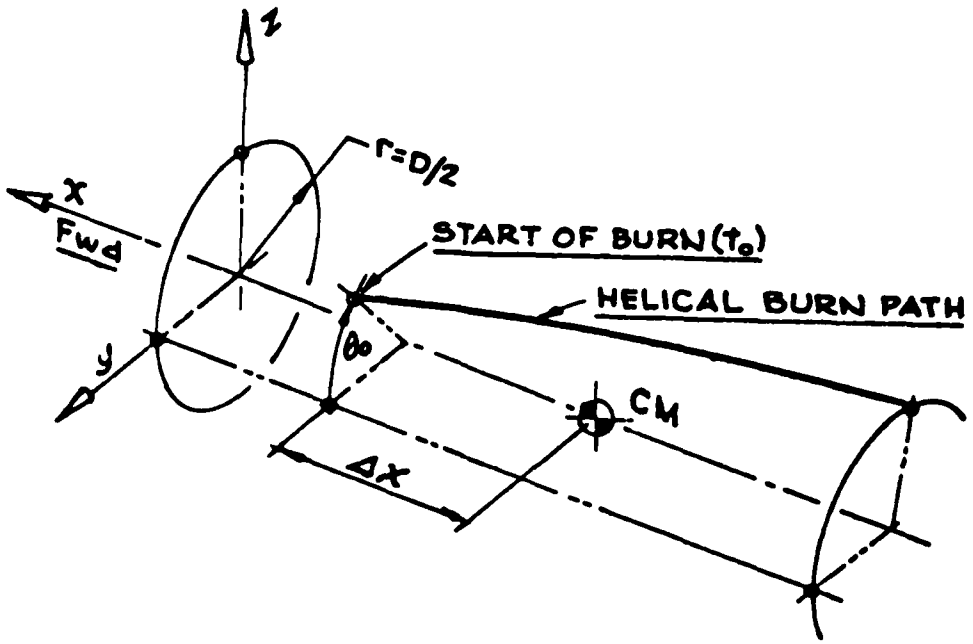

Figure 1. Helical burn path for projectile thruster

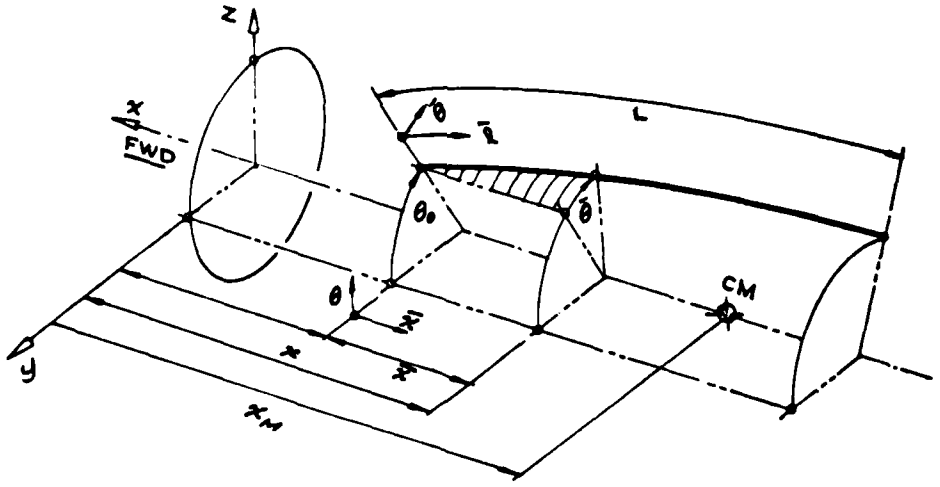

$$\bar{t}=0 \quad t=t_0 \quad \bar{t}=t-t_0$$

$$\bar{x}=0 \quad x=x_0 \quad \bar{x}=x-x_0 \quad \bar{x}=x-x_m-\Delta x$$

$$\bar{\theta}=0 \quad \theta=\theta_0 \quad \bar{\theta}=\theta-\theta_0 \quad \bar{\theta}=\frac{2\pi T}{D}\bar{x}$$

$$\bar{l}=-\bar{x}\sqrt{1+(\pi T)^2} \qquad \bar{l}^2=\bar{x}^2+(r\bar{\theta})^2$$

Figure 2. Coordinate system relationships

SYMBOLS

F	Force applied to body by burning propellant (pounds)
D	Diameter of cylindrical body section (feet)
I	Specific impulse of thruster (pound-seconds/foot of thruster)
I_x, I_y, I_z	Moments of inertia about fixed axes of body (slug-feet squared)
l	Distance down groove (feet)
L	Total length of thruster groove (feet)
N_x, N_y, N_z	Components of torque applied to body (pound-feet)
R	Linear burning rate of propellant (feet/second)
t	Time (seconds)
$\bar{t}$	Time measured from zero at start of burn (seconds)
t_c	Time t at center of thruster burn
T	Twist of helix (turns per caliber)
$\bar{x}, \bar{y}$	Coordinates of point on groove when "unwrapped" (feet)
x, y, z	Coordinates of point in body frame (feet)
θ	Polar angle of point on groove, positive from Y toward Z (radians)
τ	Time of a thruster burn (seconds)
λ	Natural frequency of solution to homogeneous differential equation (per second)
w_x, w_y, w_z	Components of spin in body frame (radians per second)

APPENDIX

PROGRAM CGSP

```
C
C    THIS IS A SAMPLE DRIVER PROGRAM FOR TESTING SUBROUTINE OMEGA
C
      COMMON R,L,I,T,D,WX,IX,IY,IZ,PI,WYZERO,WZZERO,WYZDOT,WZZDOT,
     + THZER,XZERO,FREQN,FREQF
      REAL L,I,IX,IY,IZ
C
C    DEFINITIONS
C
      R=2.2310E04
      L=1.333
      I=12.842
      T=-1.5755E-02
      D=.4199
      WX=1000.0
      IX=.136
      IY=.930
      IZ=IY
      PI=3.141592654
C
C    BURN OUT TIME. THE FOLLOWING EXACT VALUE MAY BE REPLACED
C    BY THE ACTUAL INTEGRATION CUT OFF TIME IN A NUMERICAL
C    INTEGRATION ROUTINE FOR PURPOSES OF COMPARISON.
C
      TIME = L/R
C
C    INITIAL CONDITIONS
C
      WYZERO = 0.1
      WZZERO = 0.2
C
      XZERO = 0.6667
      THZER = PI/7.
C
      CALL OMEGA(TIME,WY,WZ)
      PRINT*,'           TIME                WY                WZ'
      WRITE(*,100) TIME,WY,WZ
      WRITE(*,101)
    1 CONTINUE
      STOP
  100 FORMAT(4F15.12,//)
  101 FORMAT('1')
      END
      SUBROUTINE OMEGA(TIME,WY,WZ)
      COMMON R,L,I,T,D,WX,IX,IY,IZ,PI,WYZERO,WZZERO,WYZDOT,WZZDOT
     +   ,THZER,XZERO,FREQN,FREQF
      REAL L,I,IX,IY,IZ,J,JBAR
C
C     FREQN  =     NATURAL FREQUENCY OF THE SYSTEM
C     FREQF  =     FORCING FUNCTION FREQUENCY
```

```
C
      EL=SQRT(1. + (PI*T)*(PI*T))
      FREQN=SQRT(   (WX*WX)*(IX-IZ)*(IX-IY)/(IY*IZ)   )
      FREQF = -(2. * PI * T * R )/( D*EL )
      J=IY
      JBAR=IZ
      A=-(R*R) * I/EL
      B= R * I * XZERO
      E= -A * (( WX * (IX-IZ)/IZ)   + FREQF)
      EBAR= +A * (( WX * (IX-IY)/IY)   + FREQF)
      F= -B * (( WX * (IX-IZ)/IZ)   + FREQF)
      FBAR=  B * (( WX * (IX-IY)/IY)   + FREQF)
      DENOM= (FREQN*FREQN) - (FREQF*FREQF)
C
C CONSTANTS DERIVED  FROM THE DECOUPLING PROCESS.
C
      C1=F/(J*DENOM)
      C2B=FBAR/(JBAR*DENOM)
      C2=(A/(J*DENOM))-(E*2.*FREQF/(J*(DENOM*DENOM)))
      C1B=(A/(JBAR*DENOM))+(EBAR*2.*FREQF/(JBAR*(DENOM*DENOM)))
      C3=E/(J*DENOM)
      C4B=EBAR/(JBAR*DENOM)
      C4=0.
      C3B=0.
C
C    SUPPRESS SPURIOUS SOLUTIONS INTRODUCED BY
C    TAKING SECOND DERIVATIVES OF WY AND WZ
C
      WYZDOT = (WZZERO*WX*(IZ-IX) + B*COS(THZER))/IY
      WZZDOT = (WYZERO*WX*(IX-IY) + B*SIN(THZER))/IZ
C
C CONSTANTS DERIVED FROM THE INITIAL CONDITIONS
C
      C5= (WYZERO-C1*SIN(THZER)-C2*COS(THZER) )
      C6 = (1./FREQN)*(WYZDOT-FREQF*C1*COS(THZER)
     +   +FREQF*C2*SIN(THZER) - C3*SIN(THZER) )
      C5B= (WZZERO-C1B*SIN(THZER) -C2B*COS(THZER) )
      C6B = (1./FREQN)*(WZZDOT
     +   -FREQF*C1B*COS(THZER)+FREQF*C2B*SIN(THZER)-C4B*COS(THZER) )
C
      WY = C5*COS(FREQN*TIME) + C6*SIN(FREQN*TIME)
     +   + C1*SIN(FREQF*TIME+THZER) +
     +    C2*COS(FREQF*TIME+THZER) + C3*TIME*SIN(FREQF*TIME+THZER)
C
      WZ = C5B*COS(FREQN*TIME) + C6B*SIN(FREQN*TIME)
     +   + C1B*SIN(FREQF*TIME+THZER) + C2B*COS(FREQF*TIME+THZER)
     +   +C4B*TIME*COS(FREQF*TIME+THZER)
C
      RETURN
      END
```

Sample Execution

TIME	WY	WZ
0.000059748991	0.532756032730	-0.416309075410

DISTRIBUTION LIST

Commander
Armament Research, Development and
Engineering Center
U.S. Army Armament, Munitions
and Chemical Command
ATTN: SMCAR-MSI (5)
SMCAR-AE, B. Bushey
SMCAR-AET, W. Ebihara
SMCAR-AET-A, A. Loeb (4)
D. Mertz (10)
R. Kline (3)
E. Friedman (3)
M. Amoruso (3)
R. Campbell (3)
W. Koenig
C. Ng
H. Hudgins
E. Brown
L. Yee
SMCAR-CC, Commander/Director
S. Hirshman
SMCAR-CCL, J. Gehbauer
M. Barbarisi
SMCAR-FS, Commander/Director
T. Davidson
SMCAR-FSA-IM, S. Harnett
F. Brody
R. Hill
SMCAR-FSA-M, R. Botticelli
SMCAR-FSF, J. Lehman
SMCAR-FSN-N, C. Spinelli
J. Sacco
SMCAR-FSS, J. Gregoritis
SMCAR-FSP, F. Scerbo (4)
E. Zimpo
D. Ladd
Dover, NJ 07801-5001

Commander
U.S. Army Armament, Munitions
and Chemical Command
ATTN: AMSMC-GCL(D)
Dover, NJ 07801-5001

Administrator
Defense Technical Information Center
ATTN: Accessions Division (12)
Cameron Station
Alexandria, VA 22304-6145

Director
U.S. Army Materiel Systems
Analysis Activity
ATTN: AMXSY-MP
Aberdeen Proving Ground, MD 21005-5066

Commander
Chemical Research and Development Center
U.S. Army Armament, Munitions
and Chemical Command
ATTN: SMCCR-SPS-IL
Aberdeen Proving Ground, MD 21010-5423

Commander
Chemical Research and Development Center
U.S. Army Armament Munitions
and Chemical Command
ATTN: SMCCR-RSP-A
Aberdeen Proving Ground, MD 21010-5423

Director
Ballistic Research Laboratory
ATTN: AMXBR-OD-ST
AMXBR-BLL, C. Murphy
W. Mermagen
R. Lieske
V. Oskay
W. Sturek
Aberdeen Proving Ground, MD 21005-5066

Chief
Benet Weapons Laboratory, CCAC
Armament Research and Development Center
U.S. Army Armament, Munitions
and Chemical Command
ATTN: SMCAR-CCB-TL
Watervliet, NY 12189-5000

Commander
U.S. Army Armament, Munitions
and Chemical Command
ATTN: SMCAR-ESP-L
AMSMC-PDM
AMSMC-ASI
Rock Island, IL 61299-6000

Director
U.S. Army TRADOC Systems
Analysis Activity
ATTN: ATAA-SL
White Sands Missile Range, NM 88002

Department of the Army
ATTN: DAMA-CSM
DAMO-RQS
Washington, DC 23014

Commander
U.S. Army Material Command
ATTN: AMCDE-DM
5001 Eisenhower Avenue
Alexandria, VA 22304

Project Manager
Cannon Artillery Weapons Systems
ATTN: AMCPM-CAWS
Dover, NJ 07801-5001

Commander
Harry Diamond Laboratories
ATTN: DELHD-DCB, J. Miller
M. Probst
Adelphi, MD 20783-1197

Headquarters
Air Force Weapons Laboratory (WLX)
ATTN: Technical Library
Kirtland Air Force Base, NM 87117

Headquarters
U.S. Army Training and Doctrine Command
ATTN: ATCD-MC
ATAA-SL
Ft. Monroe, VA 23651

Director
Marine Corps Development and Engineering
Command
ATTN: Code D092
Quantico, VA 22134

Headquarters
Eglin Air Force Base
ATTN: Technical Library
Eglin Air Force Base, FL 32542

Commander
U.S. Army Test and Evaluation Command
ATTN: DRSTE-CT-T
Aberdeen Proving Ground, MD 21005

Commander
U.S. Naval Weapons Center
ATTN: Technical Library (Code 5557)
China Lake, CA 93555

Commander
U.S. Naval Surface Weapons Center
White Oak Laboratory
ATTN: Research Library
Silver Spring, MD 20910

Commander
U.S. Naval Surface Weapons Center
Dahlgren Laboratory
ATTN: Technical Library
Dahlgren, VA 22448

Commander/Director
U.S. Naval Ship Research and Development
Center
ATTN: Technical Library
Washington, DC 20007

Commanding General
U.S. Army Missile Command
ATTN: Technical Library, R. Deep
Redstone Arsenal, AL 35809

Sandia National Laboratories
Division 1631
ATTN: A. Hodapp
R. LaFarge
P.O. Box 5800
Albuquerque, NM 87185

Sandia National Laboratories
Division 8152
ATTN: D. Beyer
P.O. Box 969
Livermore, CA 94550

Raytheon Company
Missile Systems Division
ATTN: Vincent A. Grosso
Marilyn Kloss
Hartwell Rd
Bedford, MA

END

1-87

DTIC